

Article

Iprodione Removal by UV-Light-, Zero-Valent Iron- and Zero-Valent Aluminium-Activated Persulfate Oxidation Processes in Pure Water and Simulated Tertiary Treated Urban Wastewater

Bahareh Montazeri, Olga Koba-Ucun, Idil Arslan-Alaton * and Tugba Olmez-Hanci

Department of Environmental Engineering, School of Civil Engineering, Ayazaga Campus, Istanbul Technical University, Maslak, Istanbul 34469, Turkey; montazeri16@itu.edu.tr (B.M.); olgakoba24@gmail.com (O.K.-U.); tolmez@itu.edu.tr (T.O.-H.)

* Correspondence: arslanid@itu.edu.tr



Citation: Montazeri, B.; Koba-Ucun, O.; Arslan-Alaton, I.; Olmez-Hanci, T. Iprodione Removal by UV-Light-, Zero-Valent Iron- and Zero-Valent Aluminium-Activated Persulfate Oxidation Processes in Pure Water and Simulated Tertiary Treated Urban Wastewater. *Water* **2021**, *13*, 1679. <https://doi.org/10.3390/w13121679>

Academic Editors:

Jorge Rodríguez-Chueca,
Miray Bekbolet and Isabella
Natali Sora

Received: 8 March 2021

Accepted: 15 June 2021

Published: 17 June 2021

Publisher's Note: MDPI stays neutral with regard to jurisdictional claims in published maps and institutional affiliations.



Copyright: © 2021 by the authors. Licensee MDPI, Basel, Switzerland. This article is an open access article distributed under the terms and conditions of the Creative Commons Attribution (CC BY) license (<https://creativecommons.org/licenses/by/4.0/>).

Abstract: The degradation of iprodione (IPR), a once frequently used but recently banned dicarboximide fungicide, by UV-C light-, zero-valent iron- (ZVI), and zero-valent aluminium (ZVA)-activated persulfate (PS) oxidation processes was comparatively studied in distilled (pure) water (DW) and simulated, tertiary treated urban wastewater (SWW). The performance of PS-activated oxidation processes was examined by following IPR (2–10 mg/L) removal, PS (0.01–1.00 mM) consumption, metal ion release (for the two heterogeneous catalytic oxidation processes), dissolved organic carbon (DOC) removal as well as hydroxylated aromatic and low molecular weight aliphatic degradation products. The effect of pH and PS concentrations on IPR removal was examined in DW. While the experiments in DW highlighted the superior performance of UV-C/PS treatment (with 78% DOC removal after 120 min at pH = 6.2), the performance of UV-C/PS treatment decreased sharply (to 24% DOC removal after 120 min at pH = 6.8) in the complex wastewater matrix (in SWW). Complete IPR (in 20 min) and 40% DOC (in 120 min) removals were obtained with ZVI/PS treatment (1 g/L ZVI, 1.5 mM PS, pH = 3.0), which was the most effective oxidation process in SWW. The treatment performance was strongly influenced by the SWW constituents, and UV-C/PS treatment appeared to be the most sensitive to it.

Keywords: iprodione removal; UV-C-activated persulfate; zero-valent iron-activated persulfate; zero-valent aluminium-activated persulfate; performance in simulated urban wastewater

1. Introduction

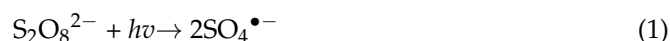
Hydantoin, or glycolylurea, is a five-membered ring heterocyclic compound with the formula $\text{CH}_2\text{C}(\text{O})\text{NHC}(\text{O})\text{NH}$ [1]. In a more general sense, hydantoins can refer to groups and a class of compounds with the same ring structure as the parent. In pharmaceuticals, hydantoin derivatives form a class of anticonvulsants: phenytoin and fosphenytoin, both of which contain hydantoin moieties and are both used as anticonvulsants in the treatment of seizure disorders [2]. One of the most important hydantoin derivatives is iprodione (IPR), which has found wide use in agricultural production as a fungicide. IPR is a dicarboximide contact fungicide with protective and curative action. It has a significant role in the control of fungal microorganisms such as *Sclerotinia*, *Botrytis*, *Rhizoctonia*, *Alternaria*, etc. [3]. In 2011, IPR's global sales reached \$115 million, accounting for a large proportion of the pesticide market [4].

Recent studies reported the presence of IPR in surface water as well as groundwater, contaminating water sources through the runoff from applied fields and/or groundwater through leaching [5–9]. IPR is a steroidogenesis inhibitor and can cause short- and long-term health effects such as atrophy and hypertrophy [10]. Furthermore, it has been reported that IPR is toxic to aquatic organisms [11], moderately toxic to small animals [12], and

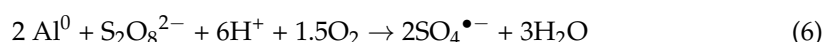
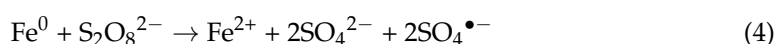
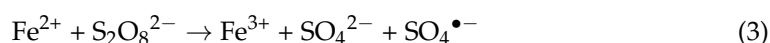
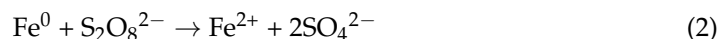
probably carcinogenic to humans [13]. In 2017, the approval of IPR was not renewed by the European Commission (EC) under EC 2017/2091 [14].

In the last three decades, advanced oxidation processes (AOPs) have been reported extensively for the removal of a wide range of micropollutants [15–18]. These processes mainly involve hydroxyl radicals (HO^\bullet) and sulfate radicals ($\text{SO}_4^{\bullet-}$) that can transform micropollutants into less harmful degradation intermediates and/or eventually mineralize them. Under appropriate conditions, AOPs can oxidize biologically resistant, toxic, and/or recalcitrant pollutants through the intermediacy of reactive oxygen species [19] though the potential formation of toxic, poor, and partial mineralization products and can be considered as a serious limitation associated with AOPs [19,20]. AOPs generally involve O_3 , H_2O_2 , and persulfate (PS) as oxidants with the assistance of UV light [16], catalysts [21], ultrasonic insertion [22], and thermal input [23]. $\text{SO}_4^{\bullet-}$ is mostly generated via two precursor salts named PS and/or peroxymonosulfate (PMS) [18] and possesses equal or even higher redox potential than HO^\bullet as well as a longer half-life [24,25].

$\text{SO}_4^{\bullet-}$ can be generated through the UV-C activation of PS wherein one mole of PS undergoes UV-C photolysis and is cleaved into two moles of $\text{SO}_4^{\bullet-}$ through the following equation [26];



Recently, catalytic activation of PS for $\text{SO}_4^{\bullet-}$ production has been reported as an advanced oxidation process to alternatively reduce toxicity and/or increase the biodegradability of wastewater [27–31]. Particularly, zero-valent iron (ZVI) and zero-valent aluminium (ZVA) activation methods have been applied to remove micropollutants from aqueous solutions [21,32]. ZVI is an effective activator of PS because of its high reactivity (reduction potential = -0.44 V vs. SHE). ZVA has also gained some attention because of its higher redox potential than ZVI (reduction potential = -1.67 V vs. SHE) to activate oxidants, including peroxides, for the degradation of a variety of contaminants in aqueous solutions [32]. The peroxide PS can be activated by ZVI (2–5) and ZVA (6) nanoparticles through the following redox reactions taking place at the metal surface as well as solution bulk [33–35];



Considering the above-mentioned urgent need for an effective treatment alternative to eliminate harmful industrial micropollutants from water/wastewater, the present study aimed at investigating the potential of one homogenous photochemical (UV-C-based) and to heterogeneous catalytic (zero-valent metal-based) PS activation processes for IPR removal from pure water and synthetic tertiary treated wastewater. These different types of oxidation systems were selected since photochemical AOPs offer the inherent advantage of highly efficient at targeting pollutants and organic carbon removal, whereas heterogeneous catalytic processes would enable catalyst separation and multiple use in real treatment applications though mass-transfer limitations would also be expected. In the first part of this study, IPR removal was examined in pure water (distilled water; DW) at varying PS concentrations and pH values employing different PS activation methods so as to optimize these processes. The treatment performances were comparatively evaluated in terms of major parameters such as IPR removal, PS consumption, and metal ion (Fe, Al) release. Furthermore, degradation products of IPR were examined by liquid chromatography (LC) for all of the studied treatment processes. Owing to the fact that the presence of different water constituents (organic as well as inorganic substances) in the reaction solution may dramatically affect the treatment performance of both homogenous photochemical and

heterogeneous catalytic oxidation processes, it is of major importance to carefully examine their performance prior to real wastewater treatment applications. Therefore, in the second part of study, UV-C/PS, ZVI/PS, and ZVA/PS processes were applied in simulated tertiary treated urban wastewater (SWW) spiked with IPR under selected/optimized treatment conditions.

2. Materials and Methods

2.1. Materials

IPR was purchased from Sigma-Aldrich (purity > 98%) (Darmstadt, Germany) and used as received. Potassium persulfate (formula: $K_2S_2O_8$; molecular weight: 270 g/mol), hydroquinone (formula: $C_6H_6O_2$; molecular weight: 110 g/mol), benzoquinone (formula: $C_6H_4O_2$; molecular weight: 108 g/mol), phenol (formula: C_6H_6O ; molecular weight: 94 g/mol), 4-chlorophenol (4-CP), 2,4-dichloroaniline (2,4-DCA), and phthalic acid (formula: $C_8H_6O_4$; molecular weight: 166 g/mol) were purchased from Sigma-Aldrich. Lactic acid (formula: $C_3H_6O_3$; molecular weight: 90 g/mol), acetic acid (formula: $C_2H_4O_2$; molecular weight: 60 g/mol), and formic acid (formula: CH_2O_2 ; molecular weight: 46 g/mol) were purchased from Merck. Catechol (formula: $C_6H_6O_2$; molecular weight: 110 g/mol) was obtained from Acros Organics. Methanol, acetic acid, sulfuric acid, and LC-MS grade water for mobile phase preparation were supplied to prepare the HPLC mobile phase. Commercial nano-scale ZVI (average particle size 50 nm; BET surface area 20–25 m^2/g ; purity > 99.5%) was obtained from Nanofer Star, Nano Iron (Czech Republic). High purity (>99.5%) ZVA nanoparticles (average particle size 100 nm; specific surface area 10–20 m^2/g) were purchased from US Research Nanomaterials, Inc. (Houston, TX, USA). All aqueous solutions were prepared in DW. In the second part of this study, the treatment performances of the UV-C/PS, ZVI/PS, and ZVA/PS processes were examined under more realistic treatment conditions, with IPR added into SWW, simulating a tertiary treated urban effluent. The composition/preparation of the SWW has been described in detail elsewhere [36].

2.2. Experimental Procedures

The UV-C/PS experiments were conducted in a LZC-ORG model (Luzchem Research Inc., Gloucester, ON, Canada) photochemical reaction chamber (dimensions: 32 × 33 × 21 cm). The photoreactor set-up and experimental procedure of the UV-C/PS are given elsewhere in detail [36]. The average radiation flux of the UV-C lamps (UV-C intensity) was measured as 0.5 W/L by a radiometer incorporated into the reaction chamber. The UV-C/PS experiments were conducted at the natural pH values of pure water and synthetic wastewater (≈ 6 –7) without pH adjustment due to the fact that according to our previous studies, this particular pH was suitable for UV-C/PS treatment, and avoiding pH adjustment is a more realistic way to treat tertiary urban effluent [36–38]. All of the ZVI/PS and ZVA/PS experiments were carried out in 500 mL-capacity borosilicate glass beakers under continuous stirring at 150 rpm to maintain the oxygen concentration of the reaction solution near saturated levels and to distribute ZVI and ZVA particles properly in the reaction solution. Experiments were carried out with 2 mg/L and 10 mg/L IPR in DW. Although this IPR concentration is much higher than environmentally relevant micropollutant concentrations reported in the scientific literature [39,40], this concentration was chosen to ensure accurate analytical, kinetic, and toxicological measurements. Furthermore, since most treatability studies dealing with the advanced oxidation of micropollutants such as IPR were conducted in the “mg/L” (ppm) concentration range, working with mg/L concentrations would enable the comparison of the present experimental results with previous related work [7,41–44]. Prior to ZVI/PS and ZVA/PS experiments, the initial pH values of the reaction solutions were adjusted to the desired, acidic value by adding 1–4 N H_2SO_4 . The selection of the acidic pH conditions for zero-valent metal-activated PS oxidation was based on former related studies in which more effective treatment performances of heterogeneous Fenton/Fenton-like reactions were reported under acidic pH (=2–5) conditions and with 1 g/catalyst concentration [21,45,46]. Therefore, after pH adjustment, 1 g/L of

ZVI (or 1 g/L of ZVA) was added to the reaction solution, and finally, PS was introduced to start reaction. Samples were taken at regular time intervals and filtered through 0.22 µm PVDF syringe filters (GVS, USA) to remove ZVI (or ZVA) particles. Additionally, the pH of the samples was increased to 7.0 by adding 1–4 N NaOH to remove the formed ferric hydroxide flocs and stop Fenton/Fenton-like reactions [21,47]. For the quantitative LC analyses, experiments were conducted in pure water (DW) with 10 mg/L IPR.

2.3. Analytical and Instrumental Procedures

IPR and its degradation products were monitored with a high-performance liquid chromatography (HPLC; Agilent 1100 Series, Agilent Technologies, Santa Clara, CA, USA) coupled with a diode array detector (G1315A, Agilent Series). IPR, 4-CP, and 2,4-DCA measurements were done at 210 nm, 280 and 240 nm, respectively, with a Nova-Pak C18 (3.9 mm × 150 mm, 4 µm, Waters, Milford, MA, USA) reversed phase column. The mobile phase consisted of 70% *v/v* methanol and 30% *v/v* ultra-pure water at a flow rate of 1 mL/min. The injection volume in the HPLC analysis and the temperature of the column were set as 100 µL and 25 °C, respectively. IPR detection and quantification limits were determined as 0.03 mg/L and 0.10 mg/L, respectively. Analytical conditions for the determination of hydroxylated degradation products of IPR including phenol, hydroquinone, *p*-benzoquinone, catechol, and phthalic acid were the following: 79.2% *v/v* ultrapure water, 19.8% *v/v* methanol, and 1.0% *v/v* acetic acid run at a flow rate of 0.8 mL/min at 270 nm, 290 nm, 245 nm, 276 nm, and 254 nm for phenol, hydroquinone, *p*-benzoquinone, catechol, and phthalic acid qualifications, respectively. The HPLC column temperature and injection volume were set as 40 °C and 40 µL, respectively. The IPR concentration was elevated from 2 mg/L to 10 mg/L during the investigation of IPR degradation products to facilitate analytical/instrument procedures.

In order to measure the released Fe and Al during the ZVI/PS and ZVA/PS treatments, 40-mL sample aliquots were taken at regular time intervals for 120 min, filtered through 0.22 µm PVDF syringe filters, and quenched immediately by adding 2 mL of freshly prepared sodium sulphite (Na₂SO₃; 10% *w/v* solution). Fe and Al were measured on a Perkin-Elmer ICP-MS (USA). For carboxylic acids (acetic acid, formic acid, and lactic acid) evolving during IPR treatment, the quantitative analysis was carried out with a Prominence LC-20A series HPLC. The analytical column (SHIM-PACK SCR-101H; 300 mm × 7.9 mm × 10 µm) was maintained at 60 °C and the mobile phase was 0.025% *v/v* H₂SO₄ run at a flow rate of 0.7 mL/min [48]. The dissolved (DOC) and total organic carbon (TOC) content of the samples was measured on a Shimadzu VPCN analyzer (Japan) equipped with an autosampler. Residual PS concentrations were determined by employing a colorimetric method [49] using a Jenway 6300 spectrophotometer (UK).

3. Results

3.1. Effect of PS Concentration

Preliminary experiments (UV-C/PS, ZVI/PS, ZVA/PS) carried out in DW spiked with 2 mg/L IPR indicated that even UV-C photolysis (UV-C intensity = 0.5 W/L; without PS addition) was capable of almost complete IPR removal (≈97%) after 120 min (Figure 1). As seen in Figure 1, the addition of PS (0.01–0.100 mM) enhanced IPR removal at all of the studied PS concentrations due to its activation by UV-C light. This increase in IPR removal can be attributed to the presence of more SO₄^{•−} that were photochemically generated at higher rates in the reaction solution upon elevation of PS concentrations. According to Figure 1, upon the addition of 0.03 mM PS to the reaction solution, IPR removal rates were significantly enhanced, resulting in complete IPR after 20 min of treatment. With the highest examined initial PS concentration of 0.100 mM PS, the time for complete IPR removal by UV-C/PS was reduced to 2 min. In other words, removal rates increased with increasing PS concentrations, and no inhibitory effects due to excessive (“overdosed”) PS concentrations were observed in the studied PS concentration range due to the fact that relatively low PS concentrations were used in this work.

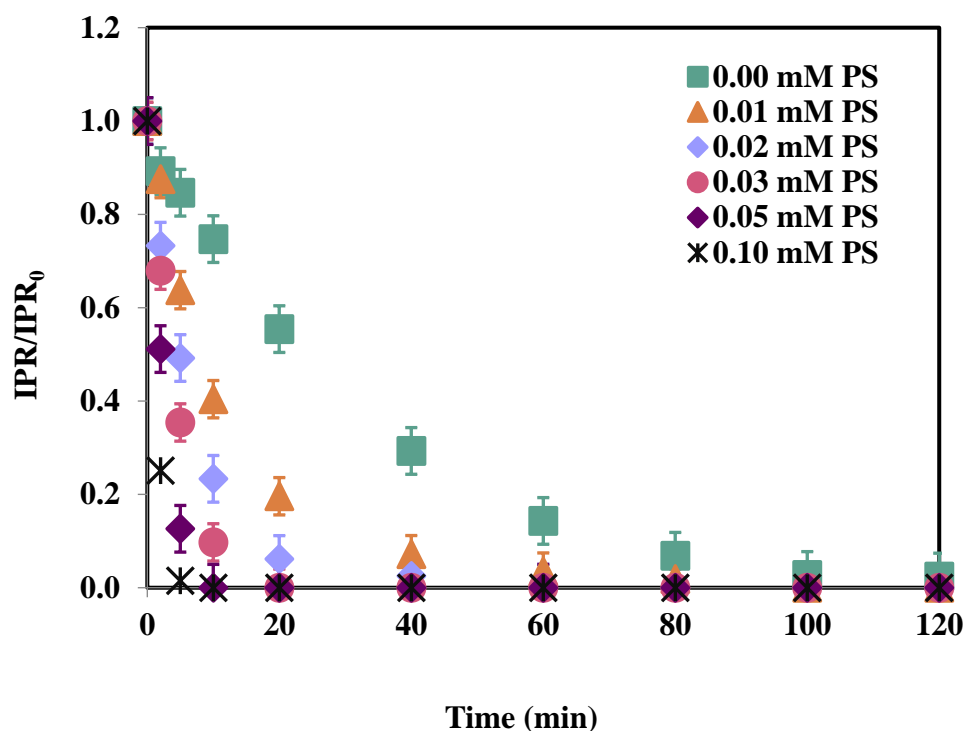


Figure 1. Changes in normalized IPR concentrations during UV-C and UV-C/PS treatments in DW at varying initial PS concentrations. IPR = 2 mg/L; UV-C intensity = 0.5 W/L; pH = 6.2.

For the heterogeneous catalytic experiments, several “control” experiments were also carried out in the absence of PS (ZVI = 1 g/L; ZVA = 1 g/L) or zero-valent metals (with PS = 1.00 mM only) at an initial concentration of 2 mg/L IPR in DW to explore IPR degradation without the activation of zero-valent metal particles or directly with PS, respectively (See Table S1). The obtained results indicated that with mere ZVI at an initial pH of 5.0 and mere ZVA at an initial pH of 3.0, IPR removals were limited to practically no removal and 35%, respectively, after 120 min of treatment (Figure 2). This observation was attributable to the higher redox potential of ZVA compared to ZVI as mentioned in the introduction section. However, it should be noted here that high reactivity (less selectivity) of ZVA compared to ZVI may be a disadvantage when working in real wastewater due to the fact that a more reactive oxidation system will more readily react with the wastewater components, causing competition reactions with the target pollutant and decreasing its removal efficiency [50,51].

Similarly, incomplete IPR removal was observed after 120 min with mere PS oxidation (data not shown), revealing that the degradation of IPR with PS was not significant and highlighting the role of ZVI or ZVA activation of PS for effective IPR removal by oxidation. Limited pollutant removals have already been reported in previous studies through the absence of catalyst or oxidant functioning as activators and/or mediators of free radical chain reactions [30,31,52–54]. For example, Zhao et al. [52], who investigated bisphenol A (BPA) removal (22 μ M) at initial pH of 6.0 by mere PS (0.1 g/L ZVI) and mere ZVI (0.2 mM PS) [52]. In their study, control experiments in the absence of ZVI or PS were conducted, and no BPA removal was obtained for the controls, indicating ZVI or PS alone could not cause BPA degradation.

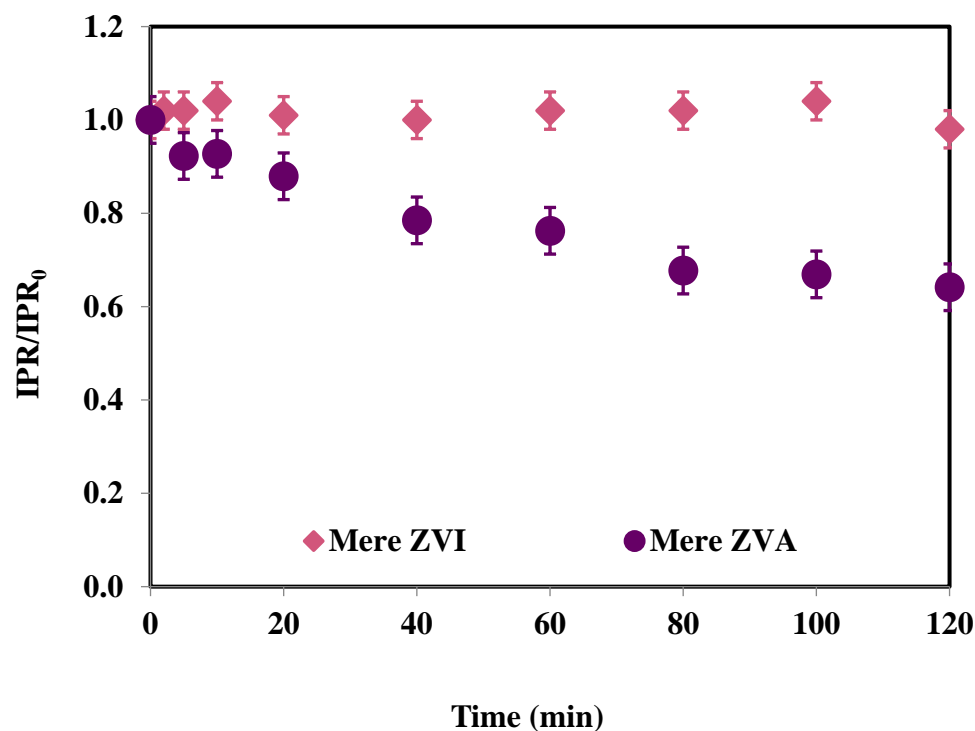


Figure 2. Changes in normalized IPR concentrations during mere ZVI treatment at an initial pH of 5.0 and mere ZVA treatment at an initial pH of 3.0. IPR = 2 mg/L; ZVI = 1 g/L; ZVA = 1 g/L.

Figure 3 depicts the effect of initial PS concentration in the range of 0.10–1.00 mM on normalized IPR removals during ZVI/PS treatment (pH = 5.0). As seen in Figure 3, practically no IPR removal (<5%) was observed after 120 min of ZVI/PS treatment in the low PS concentration range of 0.10 mM–0.25 mM. However, upon increasing the initial PS concentrations to 0.50 mM and 0.75 mM, complete IPR removal was achieved for both examined PS concentrations after 120 min of ZVI/PS treatment (see Table S2 for more details and comparison with pH = 3.0). Eventually, as the initial PS concentration was increased from 0.75 mM to 1.00 mM, the time required for complete IPR degradation decreased from 120 min to 80 min, revealing that a higher PS concentration favored IPR degradation. This could be ascribed to an increase in $\text{SO}_4^{\bullet-}$ production. This was consistent with the study reported by Wu et al. [30], who examined the performance of ZVI/PS and the effects of initial PS concentration (0.2 mM–2.5 mM PS) on atrazine removal. In that study, the degradation of 10 mg/L atrazine was affected by the PS concentration and after increasing the initial PS concentration from 0.2 mM to 0.4 mM, the atrazine removal appreciably increased from 34% to 80%. However, an inhibitory effect was evidenced at higher initial PS concentrations (1.0 mM and 2.5 mM PS), which was attributed to the generation of more $\text{SO}_4^{\bullet-}$ and its self-consumption, so excessive concentrations of PS lead to decreased atrazine removals [30]. The effect of the initial PS concentration on metoprolol, a common drug used to cure cardiovascular diseases, was investigated in the range of 0.25 mM–4.00 mM PS. In that study, the degradation of metoprolol increased from 40.2% to 96.3% as the PS concentration was increased from 0.50 mM to 3.00 mM. However, with a further increment of the initial PS concentration up to 4.00 mM, no change in metoprolol degradation was observed, probably due to the side reaction between $\text{SO}_4^{\bullet-}$ and excess PS and the self-combination of $\text{SO}_4^{\bullet-}$, causing minor improvement during the treatment process [31].

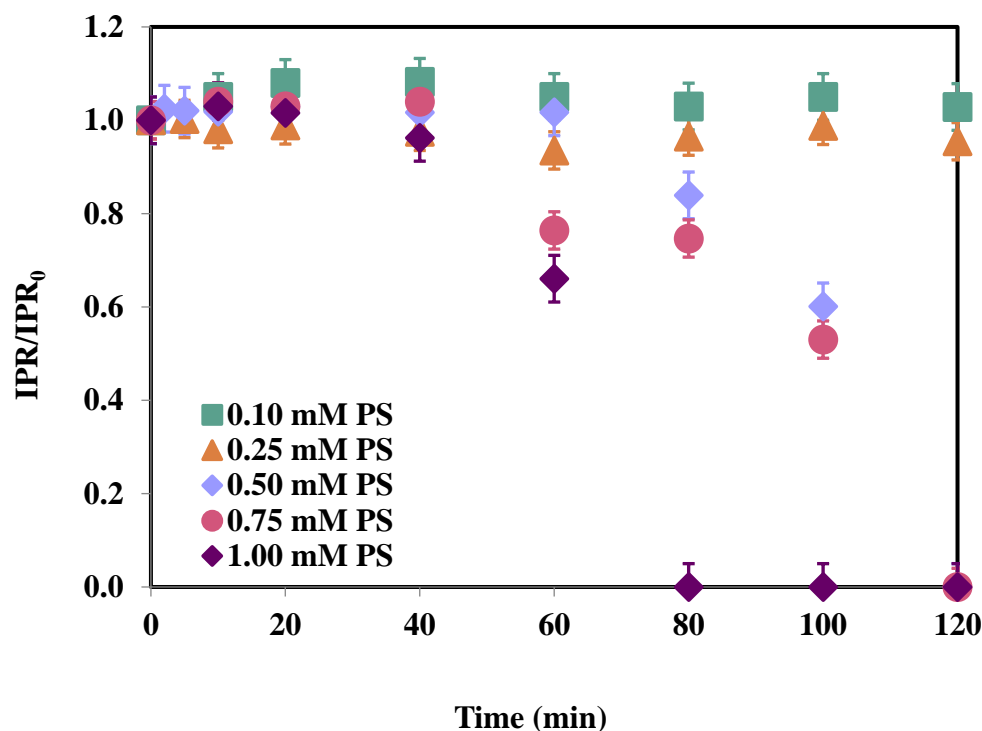
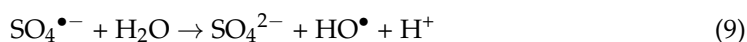


Figure 3. Changes in normalized IPR concentration during ZVI/PS treatments in DW at varying initial PS concentrations. IPR = 2 mg/L; ZVI = 1 g/L; pH = 5.0.

The effect of initial PS concentration in the range of 0.10 mM–1.00 mM PS on IPR removal rates was also examined during ZVA/PS treatment at an initial pH of 3.0 and presented in Figure 4 (see Table S3 for more details and comparison with pH = 1.5). As seen from Figure 4, IPR removal efficiencies obtained after 120 min ZVA/PS treatment with 0.10 mM and 0.25 mM PS were almost 80%. Upon increasing the initial PS concentration to 0.50 mM and 1.00 mM, complete IPR removal was observed after 120 min of treatment. This enhancement in IPR removal could be attributed to the generation of more $\text{SO}_4^{\bullet-}$, and the initial PS concentration of 1.00 mM was probably not high enough to trigger $\text{SO}_4^{\bullet-}$ scavenging reactions in the presence of excessive PS. Hence, no reduction in IPR removals were evident with increasing PS concentrations, as they had been for the UV-C/PS treatment process. Similarly, in former related work [35], the removal of 2 mg/L aqueous iopamidol solutions was examined by ZVA/PS at an initial pH of 3 in DW. In that work, the overall iopamidol removals increased from 75% for 0.25 mM and 95% for 0.50 mM treatments upon addition of 1 g/L ZVA at pH 3.0.

In another related study, the effect of PS concentration (0.20–4.00 mM) on 26.28 mg/L trichloroethylene removal through ZVA/PS was explored [55]. In that study, experimental findings revealed that the rate constants calculated for trichloroethylene were enhanced progressively from 0.0034 min^{-1} to 0.0395 min^{-1} by increasing the PS concentrations from 0.20 mM to 2.00 mM. However, the rate constants of trichloroethylene removal decreased upon further increase of the initial PS concentration due to scavenging of $\text{SO}_4^{\bullet-}$ by the excessive concentration of PS that might consume the abundant $\text{SO}_4^{\bullet-}$ generated through the following equations [55] and inhibit trichloroethylene removal:



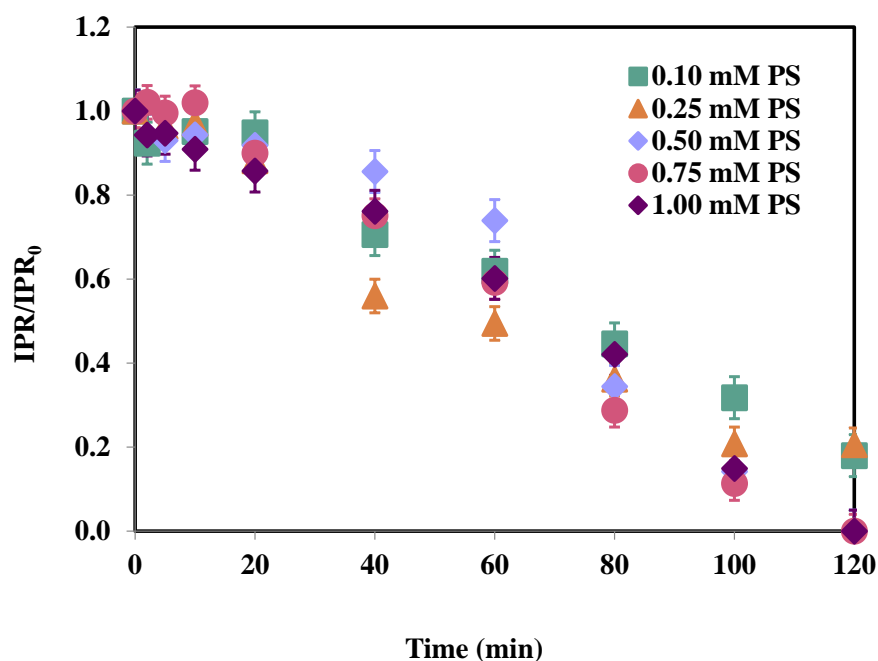


Figure 4. Changes in normalized IPR concentration during ZVA/PS treatments in DW at varying initial PS concentrations. IPR = 2 mg/L; ZVA = 1 g/L; pH = 3.0.

In summary, no $\text{SO}_4^{\bullet-}$ scavenging effects (excessive/"overdosed" PS concentrations) were observed for the examined PS concentration ranges under the present experimental conditions.

3.2. Effect of pH

Solution pH can affect the efficiency of homogenous photochemical and heterogeneous catalytic AOPs remarkably, particularly those involving metals/metal ions/oxides [32,35,50,56,57]. In the present study, no pH adjustment was carried out for the UV-C/PS treatment since in our former work, the photochemical oxidation of IPR was efficient at around neutral pH values [36–38]. In previous studies, it was demonstrated that pH affects the ZVI/PS treatment performance in the degradation of contaminants due to its catalytic activity, formation, and type of dissolved Fe species [58,59]. An acidic pH environment ($\text{pH} \leq 5$) could intensively promote the ZVI/PS system [31,45,46,60], most probably due to the accelerated ZVI corrosion that facilitates Fe^{2+} formation. In order to investigate the pH effect on IPR degradation during ZVI/PS treatment, pH values of 3.0 and 5.0 and a PS concentration of 0.50 mM were selected as shown in Figure 5 (see also Table S2). From Figure 5, it is obvious that complete IPR removal was obtained after 10 min of ZVI/PS treatment at the initial pH of 3.0, while no IPR removal was observed even after 60 min of treatment at the initial pH of 5.0. With the progress of treatment, IPR removal reached 16% and 40% after 80 min and 100 min, respectively, at pH 5.0. As is also evident in Figure 5, complete IPR removal was obtained after 120 min of ZVI/PS treatment at an initial pH of 5.0. Thus, it was concluded that IPR removals were enhanced remarkably when the pH was decreased from 5.0 to 3.0 during ZVI/PS treatment because a more acidic pH led to a more rapid corrosion of ZVI and Fe^{2+} release, resulting in faster as well as more intensive $\text{SO}_4^{\bullet-}$ generation [31,60]. The results were in agreement with Goa et al. [31], who studied ZVI/PS treatment of metoprolol in the pH range of 3.0–11.0. In that study, the maximum degradation efficiency of 99.5% was achieved at $\text{pH} = 3$ and almost 88.7% metoprolol had degraded within the first 5 min. By increasing the pH from 5 to 9, the degradation of metoprolol decreased from 95.9% to 83.8% [31].

Since acidic pH conditions facilitate the removal of organic pollutants and are essential for metal-based catalytic treatment processes [32,35,50,61,62], the pH values of 3.0 and

1.5 were tested for the ZVA/PS treatment system (with 0.50 mM PS). Figure 6 depicts the effect of the initial pH on IPR degradation with ZVA/PS at an initial PS concentration of 0.50 mM (see also Table S3). As apparent from Figure 6, IPR degradation was appreciably faster at pH = 1.5 compared to pH = 3.0 during the first 60 min of ZVA/PS treatment. This was attributed to the fact that the reactivity of ZVA might be enhanced through the rapid corrosion of ZVA, and the continuous activation of the passive layer in the solution with a higher H^+ concentration (pH = 1.5) [50]. However, with the progress of the treatment (after 60 min), both treatments resulted in similar IPR removal rates.

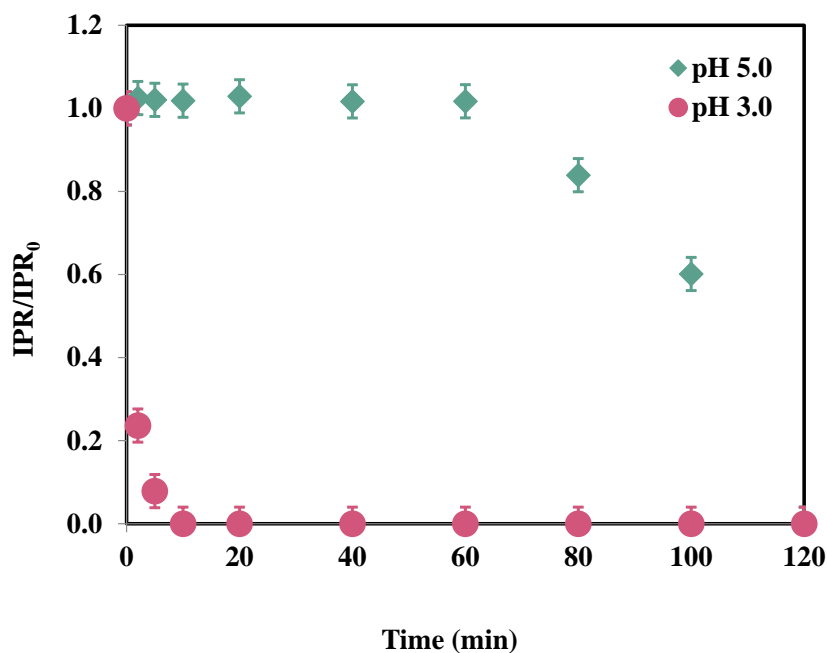


Figure 5. Changes in normalized IPR concentration during ZVI/PS treatments in DW at varying initial pH values. IPR = 2 mg/L; PS = 0.50 mM; ZVI = 1 g/L.

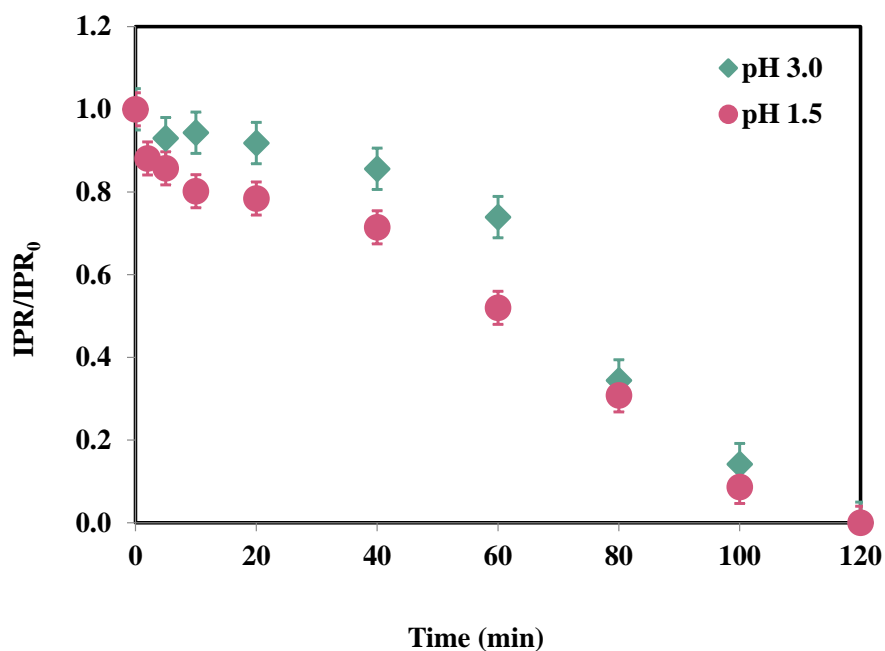


Figure 6. Changes in normalized IPR concentration during ZVA/PS treatments in DW at varying initial pH values. IPR = 2 mg/L; PS = 0.50 mM; ZVA = 1 g/L.

3.3. Metal (Fe, Al) Release and PS Consumption for Heterogeneous Oxidation Processes

For heterogeneous catalytic oxidation systems, metal ion release and PS consumption were also assessed to further examine their treatment mechanism. The degree of Fe release and PS consumption was followed during the ZVI/PS (PS = 0.50 mM, pH = 3.0) treatment of 2 mg/L IPR in DW (see Table S4 for more details). According to Table 1, complete IPR degradation was achieved during the first 10 min of the ZVI/PS treatment together with 13% of PS consumption. As also seen in Table 1, more ZVI surface corrosion resulted in more Fe release from the ZVI surface to the reaction bulk and consequently led to a higher PS consumption for $\text{SO}_4^{\bullet-}$ generation. The ultimately released Fe concentration was measured as 129 $\mu\text{g/L}$, where almost complete IPR degradation and PS consumption were achieved. Fe concentrations positively correlated with PS consumption and pollutant removals during the ZVI/PS treatment.

Table 1. IPR abatement, Fe release and PS consumption observed during ZVI/PS treatment of IPR. IPR = 2 mg/L; PS = 0.50 mM; ZVI = 1 g/L; pH = 3.0.

Time (min)	IPR (mg/L)	Fe ($\mu\text{g/L}$)	PS Consumption (%)
5	0.16	<10	10
10	0	<10	13
30	0	<10	20
60	0	88	68
120	0	129	95

Table 2 presents the IPR and released Al concentrations as well as PS consumption during the ZVA/PS (PS = 0.50 mM; pH = 3.0) treatment of 2 mg/L IPR in DW (see Table S5 for more details). According to the Al ion measurements from Table 2, it was evident that fast Al release being observed throughout the entire IPR treatment period could be attributed to the acidic pH environment that hindered ZVA passivation so that continuous $\text{SO}_4^{\bullet-}$ and/or HO^{\bullet} formation and subsequent pollutant degradation occurred via Fenton-like redox reactions [51].

Table 2. IPR abatement, Al release, and PS consumption observed during ZVA/PS treatment of IPR. IPR = 2 mg/L; PS = 0.50 mM; ZVA = 1 g/L; pH = 3.0.

Time (min)	IPR (mg/L)	Al ($\mu\text{g/L}$)	PS Consumption (%)
5	1.90	-	-
10	1.87	299	5
30	1.79	324	7
60	1.49	353	10
120	0	499	15

3.4. Degradation Products and Mineralization Rates

As aforementioned, $\text{SO}_4^{\bullet-}$ are generated by the activation of PS with ZVI [63]. Unlike the metal ion activation of PS, where excessive concentrations of ferrous salts are necessary and might even react with $\text{SO}_4^{\bullet-}$, ZVI can slowly and continuously release ferrous ions to activate PS [63]. In the present study, some IPR degradation products were measured during PS-activated oxidation processes, including ZVI/PS treatment in DW. Figure 7 shows changes in the IPR and DOC (a), hydroquinone (b), carboxylic acids (lactic, acetic acids), and (c) concentrations during the ZVI/PS (PS = 2.50 mM) treatment of 10 mg/L IPR in DW in the initial solution pH of 3.0. As seen in Figure 7a, almost complete IPR removal was achieved after 20 min of ZVI/PS treatment. Prolonged ZVI/PS treatment led to only 21% DOC removal after 120 min, suggesting the formation of intermediates being rather resistant to ultimate oxidation. Formation of 2,4-DCA, 4-CP, catechol, *p*-benzoquinone, phenol, formic acid, and phthalic acid were investigated as possible degradation intermediates during the ZVI/PS treatment of IPR; however, none of them could be detected by LC

analysis under the selected reaction conditions. Hydroquinone was identified after 90 of min ZVI/PS treatment as 0.44 mg/L, reaching its highest concentration of 0.50 mg/L after 120 min of treatment. Acetic and lactic acid at concentrations of 34.3 mg/L and 16.85 mg/L could be determined after 20 min and 40 min of ZVI/PS treatment, respectively (Figure 7c). Although the concentration of acetic acid gradually increased to 79.6 mg/L after 120 of min treatment, lactic acid concentration remained practically stable until the end of the treatment.

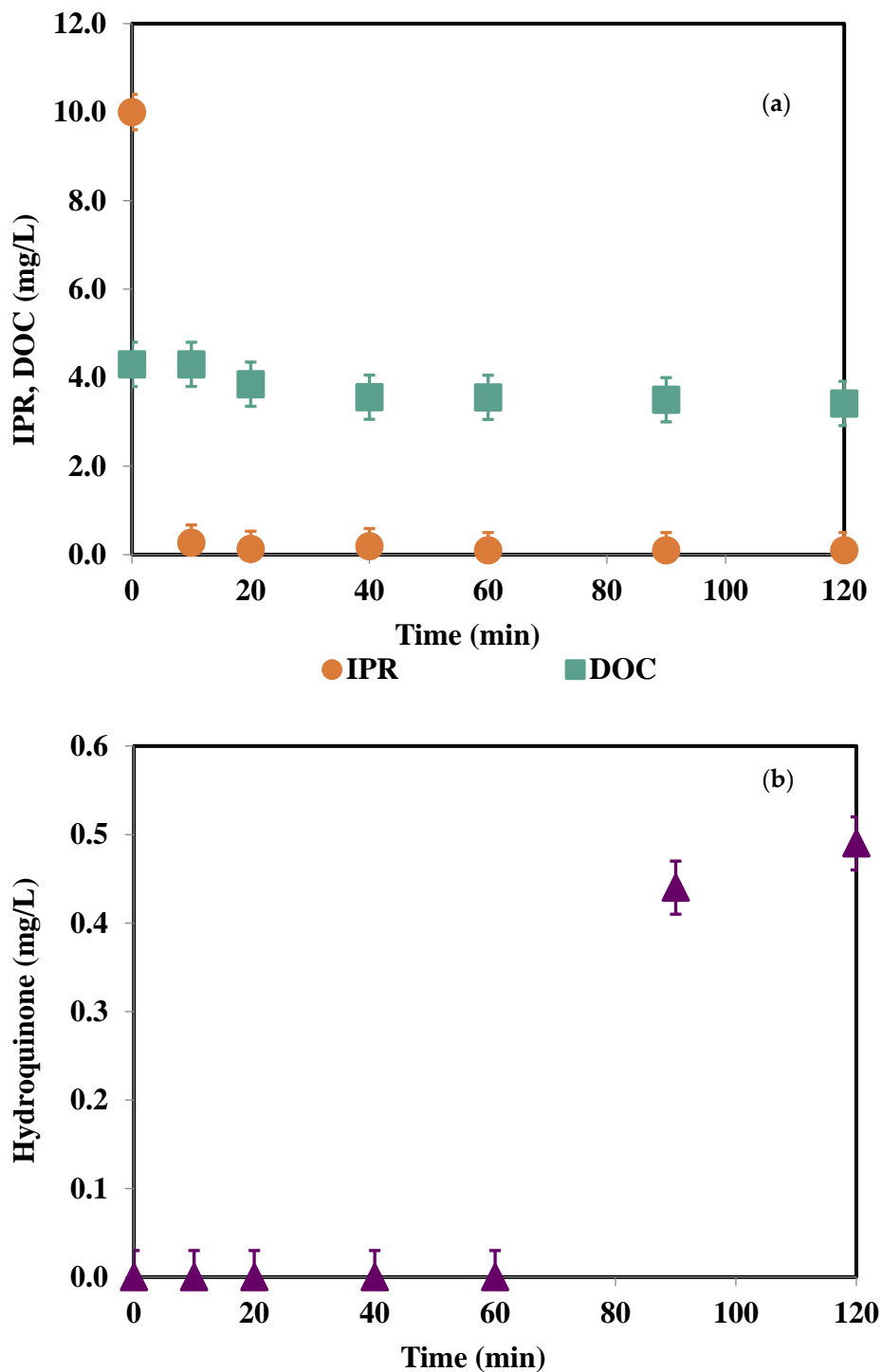


Figure 7. Cont.

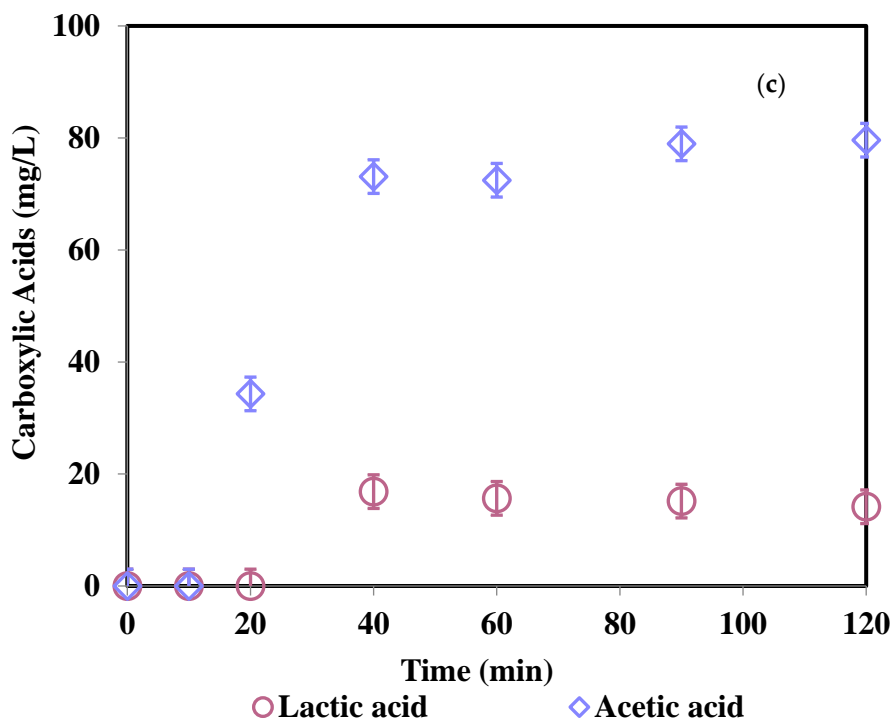


Figure 7. Changes in IPR and DOC (a), hydroquinone (b) and carboxylic acids (c) concentrations during ZVI/PS treatment. IPR = 10 mg/L; PS = 2.50 mM; ZVI = 1 g/L; pH = 3.0.

Identification IPR degradation products during photochemical treatment were also carried out by HPLC. Figure S1 in the Supplementary Materials Section depicts changes in IPR and DOC (a), 2,4-DCA (b), and carboxylic acids (c) concentrations during UV-C/PS (PS = 0.30 mM; pH = 6.2) treatment of 10 mg/L IPR in DW. From Figure S1 (see Supplementary Materials section) it is evident that UV-C/PS treatment was effective both in terms of IPR and mineralization resulting in complete IPR and 78% DOC removal after 120 min of UV-C/PS treatment. As seen in Figure S1, in the first 2 min of the IPR treatment with UV-C/PS, rapid 2,4-DCA formation was evident, most likely as a result of C-N bond cleavage. 2,4-DCA disappeared after 20 min of photochemical treatment. 2,4-DCA formation as one of the most common degradation intermediates of IPR degradation was reported previously in related work [64,65]. With the progress of photochemical treatment, hydroquinone (HQ), as one of the most common hydroxylated addition intermediates of aromatic organics, could be quantified at $t = 20$ min and $t = 60$ min as 0.050 mg/L and 0.064 mg/L, respectively. HQ disappeared after 120 min of UV-C/PS treatment. Acetic and formic acid could be detected as the low molecule weight organic acid end products.

Figure S2 in the Supplementary Materials section shows changes in normalized IPR (a) and DOC (b) concentrations during the ZVA/PS (PS = 2.50 mM; pH = 3.0) treatment of 10 mg/L IPR in DW. The insert in Figure S2a displays PS consumption (%) during the ZVA/PS treatment of 10 mg/L IPR in DW. From Figure S2 it is evident that for the first 60 min ZVA/PS treatment, IPR removal was very slow, and only 12% IPR removal was achieved together with 25% PS consumption. With the progress of the treatment, IPR removal continued and reached 65% after 120 min of treatment together with 33% PS consumption and poor mineralization. The observed poor PS consumption (33%) during 120 min of the ZVA/PS treatment of IPR can be explained by considering that IPR degradation was attributed not only to $\text{SO}_4^{\bullet-}$ but also to HO^{\bullet} derived from the reaction of H_2O with $\text{SO}_4^{\bullet-}$ as well as single electron transfer from ZVA to O_2 [65]. However, due to the lower diffusion rate of O_2 , whether O_2 was involved in the reaction depended upon the degree of ZVA corrosion [55].

Identification of the above-mentioned oxidation intermediates was also investigated for the ZVA/PS treatment of IPR, however, none of them could be detected.

3.5. Experiments in Simulated Tertiary Wastewater

In order to elucidate the oxidation of IPR in a more complex effluent matrix by UV-C and zero-valent metal activated PS (UV-C/PS, ZVI/PS ZVA/PS treatments), additional experiments were conducted in a wastewater sample mimicking tertiary treated urban wastewater (called SWW herein). In addition, DOC removals were also investigated to study the fate of organic matter originating from IPR and its degradation products. Figure 8 presents changes in normalized IPR (a) and DOC (b) abatements through UV-C/PS (PS = 0.09 mM) treatments for 2 mg/L IPR-spiked SWW. The removal of IPR with UV-C/PS treatment was complete after 80 min, whereas DOC removal was limited to only 24% after 120 min treatment. Apparently, UV-C/PS (PS = 0.09 mM) treatment was very sensitive to the SWW components and hence not capable of efficient DOC removal in more a complex matrix compared to DW. The ingredients of SWW (inorganic ions, organic matter) might compete with PS for UV-C light absorption, eventually leading to fewer available photons to generate $\text{SO}_4^{\bullet-}$ [66].

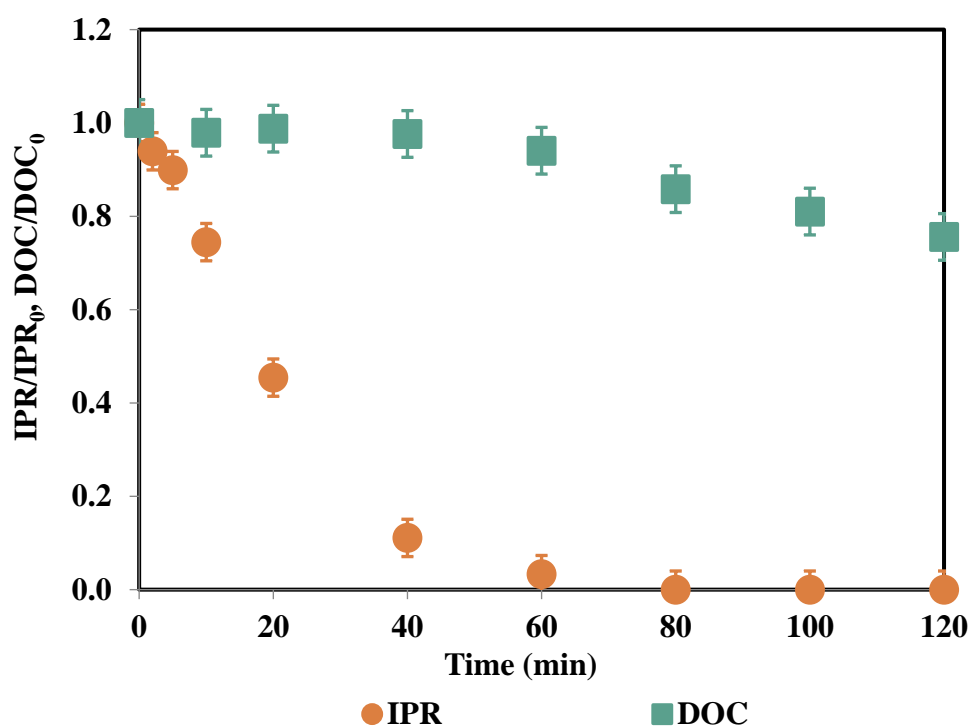


Figure 8. Changes in normalized IPR and DOC during UV-C/PS treatments in SWW. IPR = 2 mg/L; PS = 0.09 mM; DOC = 11.4 mg/L; UV-C intensity = 0.5 W/L; pH = 6.8 (the pH of SWW).

Figure 9 shows changes in normalized IPR and DOC values by ZVI/PS (PS = 1.50 mM) treatment at pH 3.0 with 2 mg/L IPR in SWW (see Table S6 for more details). From Figure 9, it is evident that IPR was completely removed after 20 min of ZVI/PS treatment together with 30% of DOC. Beyond this treatment time, no further DOC removal was observed. As seen in Figure 9, prolonged ZVI/PS treatment led to only 40% DOC reduction after 120 min.

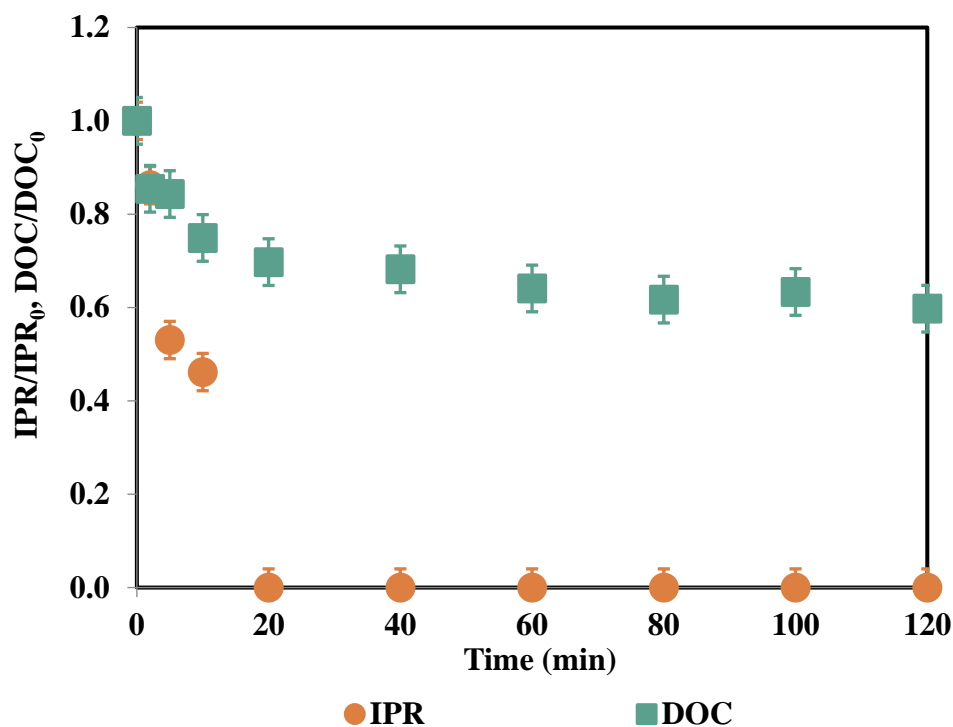


Figure 9. Changes in normalized IPR and DOC during ZVI/PS treatments in SWW. IPR = 2 mg/L; DOC = 11.4 mg/L; PS = 1.50 mM; ZVI = 1 g/L, pH = 3.0.

Experiments in SWW indicated that complete IPR removal was achieved only after 120 min of ZVA/PS treatment. Figure 10 shows changes in normalized IPR and DOC values with ZVA/PS (PS = 1.50 mM; pH = 3.0) for 2 mg/L IPR treatment in SWW. From Figure 10, it is evident that no IPR removal occurred during the 120 min of ZVA/PS treatment of the SWW spiked with 2 mg/L IPR, while at the initial PS concentration of 0.50 mM, complete IPR removal was obtained in DW after 120 min. This observation could be ascribed to the complexity of SWW (the presence of various inorganic and organic compounds) compared to DW [51]. The inhibition of IPR removal in SWW was stronger during ZVA/PS treatment compared to ZVI/PS treatment [51,67]. This observation could be attributed to the following: ZVA is more active than ZVI and hence more readily undergoes redox reactions. This higher reactivity of ZVA means lower selectivity so that in a complex wastewater matrix/in the presence of a variety of organic/inorganic constituents, the more reactive oxidant ZVA will not be used efficiently for the removal of the target pollutant and its degradation products. Moreover, when Fe is involved in redox reactions, additional removal mechanisms could play a role in the reaction solution [32,56,67]; in other words, other types of reaction routes are possible. Fe has two oxidation states—Fe(II) and Fe(III)—that can undergo a series of redox (Fenton and Fenton-like oxidation) and complexation reactions with the SWW constituents. For instance, Fe complexation of iprodione's transformation products could enhance their oxidation by changing the solubility and availability of these substrates towards active oxidants [50,57,67]. In this way, the removal of iprodione and its organic carbon content would be more effective with ZVI. It should also be noted here that ZVA is more active at a very acidic pH (=1.5); however, very acidic pH values are not realistic conditions for wastewater treatment. At pH = 3.0, which was selected as the reaction pH for heterogeneous catalytic treatment in SWW, its performance is expected to decrease sharply.

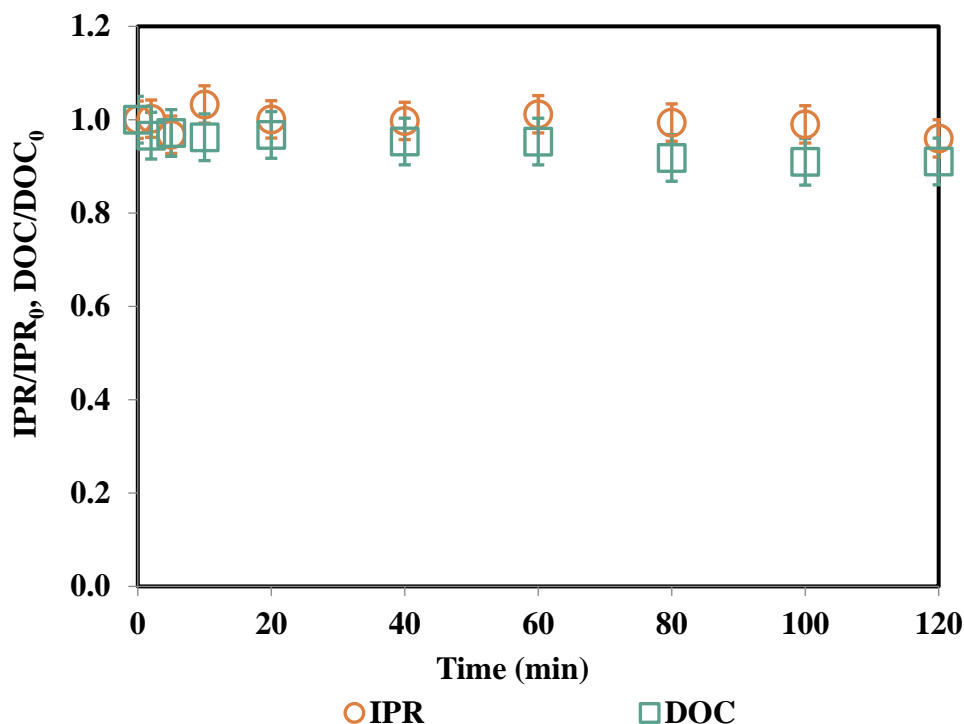


Figure 10. Changes in normalized IPR and DOC during ZVA/PS treatments in SWW. IPR = 2 mg/L; DOC = 11.96 mg/L; PS = 1.50 mM; ZVA = 1 g/L, pH = 3.0.

Changes in normalized DOC values IPR-spiked SWW were also followed during 120 min ZVA/PS treatment at pH 3.0 (see Table S7 for more details). In former related work [35], it was demonstrated that the presence of organic and inorganic compounds in wastewater samples such as humic acid (a major dissolved organic matter component in water/wastewater samples), had an inhibitory effect on the performance of the ZVA/PS oxidation system such that no iopamidol removal was observed during ZVA/PS treatment in the wastewater sample [35]. As seen in Figure 10, practically no change in normalized DOC was observed (9%), indicating that the ingredients present in SWW might inhibit the oxidation process.

4. Conclusions

PS activation methods have recently gained an immense interest in micropollutant removal using sulfate-radical based advanced oxidation processes. In the present study, the degradation of IPR, a once commercially important fungicide identified as a potential carcinogen/endocrine disrupting compound and hence banned via regulation, was comparatively investigated employing one homogenous photochemical and two heterogeneous catalytic oxidation processes, namely UV-C/PS and ZVI/PS-ZVA/PS treatments, respectively. A series of treatability experiments were first y conducted at varying PS concentrations and pH values to examine the effect of these critical parameters on IPR removal in pure water. Moreover, degradation products of IPR were quantified in order to comparatively examine the reaction routes/mechanisms of the UV-C/PS, ZVI/PS and ZVA/PS treatment processes. IPR removal was also examined in simulated tertiary treated urban wastewater (SWW) under specific reaction conditions to elucidate the performance of the PS-activated oxidation systems in a real wastewater environment. UV-C/PS (PS = 0.09 mM; pH = 6.8) treatment of IPR in SWW resulted in complete IPR (in 80 min) and 24% DOC removal after 120 min, whereas ZVI/PS (PS = 1.50 mM; pH = 3.0) treatment exhibited faster IPR removal (in 20 min) together with 40% DOC removal after 120 min in SWW, revealing that the photochemical treatment process was more sensitive to the complex effluent matrix.

Neither IPR removal nor DOC removals were obtained during ZVA/PS treatment in SWW, indicating that the presence of various organic and inorganic compounds in SWW seriously hindered and inhibited IPR removal with the more active/reactive ZVA/PS treatment system. From the experimental results it was evident that those treatment processes showing superior treatment performance in pure water (DW), could result in a relatively poor treatment performance when applied in a simulated, complex wastewater matrix (SWW) due to their high reactivity (ZVA/PS), selectivity, and/or sensitivity (UV-C/PS). Considering the experimental findings of this study, the ZVI/PS treatment process may be offered as a more feasible treatment option for the efficient removal of industrial micropollutants found in water or wastewater. However, the economic feasibility and ecotoxicological safety of this heterogeneous iron-based catalytic treatment system should be further investigated in more detail before real-scale application could be envisioned.

Supplementary Materials: The following are available online at <https://www.mdpi.com/article/10.3390/w13121679/s1>: Figure S1: Changes in IPR and DOC (a), 2,4-DCA (b) and carboxylic acids (c) concentrations during UV-C/PS treatment of IPR in DW. IPR = 10 mg/L; PS = 0.30 mM; DOC of 10 mg/L IPR = 4.3 mg/L; UV-C intensity = 0.5 W/L; pH = 6.2. Figure S1 (a) insert gives the calculated PS consumptions (%) during UV-C/PS treatment of 10 mg/L IPR in DW. Figure S2: Changes in normalized IPR (a) and DOC (b) values during ZVA/PS treatment in DW. IPR = 10 mg/L; PS = 2.50 mM; DOC for 10 mg/L IPR = 4.3 mg/L; ZVA = 1 g/L; pH = 3.0. Figure S2 (a) insert indicates the calculated PS consumptions (%) during ZVA/PS treatment of 10 mg/L IPR in DW. Table S1: IPR removals obtained during mere ZVI treatment at an initial pH of 5.0, mere ZVA treatment at an initial pH of 3.0 as well as mere PS treatment of IPR at pH = 6.2. IPR = 2 mg/L; ZVI = 1 g/L; ZVA = 1 g/L; PS = 1.00 mM. Table S2: IPR removals obtained during ZVI/PS treatment in DW. IPR = 2 mg/L; ZVI = 1 g/L. Table S3: IPR removals obtained during ZVA/PS treatments in DW. IPR = 2 mg/L; ZVA = 1 g/L. Table S4: IPR and DOC removals as well as PS consumptions obtained during ZVI/PS treatment in DW. IPR = 10 mg/L; DOC = 4.3 mg/L; PS = 2.50 mM; ZVI = 1 g/L; pH = 3.0. Table S5: IPR and DOC removals as well as PS consumptions during ZVA/PS treatment in DW. IPR = 10 mg/L; PS = 2.50 mM; DOC for 10 mg/L IPR = 4.3 mg/L; ZVA = 1 g/L; pH = 3.0. Table S6: IPR and DOC removals as well as PS consumptions during ZVI/PS treatments in SWW. IPR = 2 mg/L; DOC = 11.4 mg/L; PS = 1.50 mM; ZVI = 1 g/L, pH = 3.0. Table S7: IPR and DOC removals as well as PS consumptions during ZVA/PS treatments in SWW. IPR = 2 mg/L; DOC = 11.96 mg/L; PS = 1.50 mM; ZVA = 1 g/L, pH = 3.0.

Author Contributions: Conceptualization, I.A.-A. and T.O.-H.; methodology, I.A.-A. and T.O.-H.; software, B.M.; validation, B.M. and O.-K.U.; formal analysis, O.-K.U. and I.A.-A.; investigation, I.A.-A.; resources, I.A.-A.; data curation, B.M. and O.-K.U.; writing—original draft preparation, B.M.; writing—review and editing, I.A.-A.; visualization, B.M.; supervision, I.A.-A.; project administration, I.A.-A.; funding acquisition, I.A.-A. All authors have read and agreed to the published version of the manuscript.

Funding: This research was funded by the Istanbul Technical University under Grant Nr. MDK-2019-42052.

Institutional Review Board Statement: Not applicable.

Informed Consent Statement: Not applicable.

Data Availability Statement: The data presented in this study are available on request from the corresponding author.

Conflicts of Interest: The authors declare no conflict of interest.

References

1. Shimizu, T. Studies on the Use of Hydantoin-Related Compounds as Slow Release Fertilizers. *Soil Sci. Plant Nutr.* **1986**, *32*, 373–382. [[CrossRef](#)]
2. Belafdal, O.; Bergon, M.; Calmon, J.P. Mechanism of hydantoin ring opening in iprodione in aqueous media. *Pestic. Sci.* **1986**, *17*, 335–342. [[CrossRef](#)]
3. Andrioli, N.B.; Chaufan, G. Dose-independent genotoxic response in A549 cell line exposed to fungicide Iprodione. *Arch. Toxicol.* **2021**, *95*, 1071–1079. [[CrossRef](#)]

4. Wei, Y.; Meng, Y.; Huang, Y.; Liu, Z.; Zhong, K.; Ma, J.; Zhang, W.; Li, Y.; Lu, H. Development toxicity and cardiotoxicity in zebrafish from exposure to iprodione. *Chemosphere* **2021**, *263*, 127860. [[CrossRef](#)]
5. Derbalah, A.; Nakatani, N.; Sakugawa, H. Distribution, seasonal pattern, flux and contamination source of pesticides and nonylphenol residues in Kurose River water, Higashi-Hiroshima, Japan. *Geochem. J.* **2003**, *37*, 217–232. [[CrossRef](#)]
6. Sequinatto, L.; Reichert, J.M.; Dos Santos, D.R.; Reinert, D.J.; Copetti, A.C.C. Occurrence of agrochemicals in surface waters of shallow soils and steep slopes cropped to tobacco. *Química Nova* **2013**, *36*, 768–772. [[CrossRef](#)]
7. Garbin, J.R.; Milori, D.; Simões, M.L.; da Silva, W.T.; Neto, L.M. Influence of humic substances on the photolysis of aqueous pesticide residues. *Chemosphere* **2007**, *66*, 1692–1698. [[CrossRef](#)] [[PubMed](#)]
8. Zhang, M.; Wang, W.; Zhang, Y.; Teng, Y.; Xu, Z. Effects of fungicide iprodione and nitrification inhibitor 3, 4-dimethylpyrazole phosphate on soil enzyme and bacterial properties. *Sci. Total Environ.* **2017**, *599–600*, 254–263. [[CrossRef](#)] [[PubMed](#)]
9. Sauret-Szczepanski, N.; Mirabel, P.; Wortham, H. Development of an SPME–GC–MS/MS method for the determination of pesticides in rainwater: Laboratory and field experiments. *Environ. Pollut.* **2006**, *139*, 133–142. [[CrossRef](#)]
10. Bernardes, P.M.; Andrade-Vieira, L.F.; Aragão, F.B.; Ferreira, A.; Ferreira, M.F.D.S. Toxicological effects of commercial formulations of fungicides based on procymidone and iprodione in seedlings and root tip cells of *Allium cepa*. *Environ. Sci. Pollut. Res.* **2019**, *26*, 21013–21021. [[CrossRef](#)] [[PubMed](#)]
11. Radice, S.; Ferraris, M.; Marabini, L.; Grande, S.; Chiesara, E. Effect of iprodione, a dicarboximide fungicide, on primary cultured rainbow trout (*Oncorhynchus mykiss*) hepatocytes. *Aquat. Toxicol.* **2001**, *54*, 51–58. [[CrossRef](#)]
12. Blystone, C.R.; Lambright, C.S.; Furr, J.; Wilson, V.S.; Grayjr, L.E., Jr. Iprodione delays male rat pubertal development, reduces serum testosterone levels, and decreases ex vivo testicular testosterone production. *Toxicol. Lett.* **2007**, *174*, 74–81. [[CrossRef](#)]
13. Dabrowski, J.M.; Shadung, J.M.; Wepener, V. Prioritizing agricultural pesticides used in South Africa based on their environmental mobility and potential human health effects. *Environ. Int.* **2014**, *62*, 31–40. [[CrossRef](#)] [[PubMed](#)]
14. European Commission (EC). *Regulation EU 2091 Concerning the Non-Renewal of Approval of the Active Substance Iprodione, in Accordance with Regulation (EC) No 1107/2009 of the European Parliament and of the Council Concerning the Placing of Plant Protection Products on the Market, and Amending Commission Implementing Regulation (EU) No 540/2011*; Official Journal of the European Union: Brussels, Belgium, 2017; pp. 25–27.
15. Wang, J.; Zhuan, R. Degradation of antibiotics by advanced oxidation processes: An overview. *Sci. Total Environ.* **2020**, *701*, 135023. [[CrossRef](#)] [[PubMed](#)]
16. Yang, Q.; Ma, Y.; Chen, F.; Yao, F.; Sun, J.; Wang, S.; Yi, K.; Hou, L.; Li, X.; Wang, D. Recent advances in photo-activated sulfate radical-advanced oxidation process (SR-AOP) for refractory organic pollutants removal in water. *Chem. Eng. J.* **2019**, *378*, 122149. [[CrossRef](#)]
17. Wang, J.L.; Xu, L.J. Advanced Oxidation Processes for Wastewater Treatment: Formation of Hydroxyl Radical and Application. *Crit. Rev. Environ. Sci. Technol.* **2012**, *42*, 251–325. [[CrossRef](#)]
18. Waclawek, S.; Lutze, H.V.; Grübel, K.; Padil, V.V.T.; Černík, M.; Dionysiou, D.D. Chemistry of persulfates in water and wastewater treatment: A review. *Chem. Eng. J.* **2017**, *330*, 44–62. [[CrossRef](#)]
19. Dewil, R.; Mantzavinos, D.; Poullos, I.; Rodrigo, M.A. New perspectives for Advanced Oxidation Processes. *J. Environ. Manag.* **2017**, *195*, 93–99. [[CrossRef](#)]
20. Cuerda-Correa, E.M.; Alexandre-Franco, M.F.; Fernández-González, C. Advanced Oxidation Processes for the Removal of Antibiotics from Water: An Overview. *Water* **2020**, *12*, 102. [[CrossRef](#)]
21. Xiao, S.; Cheng, M.; Zhong, H.; Liu, Z.; Liu, Y.; Yang, X.; Liang, Q. Iron-mediated activation of persulfate and peroxymonosulfate in both homogeneous and heterogeneous ways: A review. *Chem. Eng. J.* **2020**, *384*, 123265. [[CrossRef](#)]
22. Chen, W.-S.; Su, Y.-C. Removal of dinitrotoluenes in wastewater by sono-activated persulfate. *Ultrason. Sonochem.* **2012**, *19*, 921–927. [[CrossRef](#)] [[PubMed](#)]
23. Liang, C.; Su, H.-W. Identification of Sulfate and Hydroxyl Radicals in Thermally Activated Persulfate. *Ind. Eng. Chem. Res.* **2009**, *48*, 5558–5562. [[CrossRef](#)]
24. Kolthoff, I.M.; Miller, I.K. The Chemistry of Persulfate. I. The Kinetics and Mechanism of the Decomposition of the Persulfate Ion in Aqueous Medium. *J. Am. Chem. Soc.* **1951**, *73*, 3055–3059. [[CrossRef](#)]
25. Buxton, G.V.; Greenstock, C.L.; Helman, W.P.; Ross, A.B. Critical Review of rate constants for reactions of hydrated electrons, hydrogen atoms and hydroxyl radicals (OH/O⁻ in Aqueous Solution. *J. Phys. Chem. Ref. Data* **1988**, *17*, 513–886. [[CrossRef](#)]
26. Dogliotti, L.; Hayon, E. Flash photolysis of per[oxydi]sulfate ions in aqueous solutions. The sulfate and ozonide radical anions. *J. Phys. Chem.* **1967**, *71*, 2511–2516. [[CrossRef](#)]
27. Kim, C.; Ahn, J.-Y.; Kim, T.Y.; Shin, W.S.; Hwang, I. Activation of Persulfate by Nanosized Zero-Valent Iron (NZVI): Mechanisms and Transformation Products of NZVI. *Environ. Sci. Technol.* **2018**, *52*, 3625–3633. [[CrossRef](#)]
28. Pang, Y.; Zhou, Y.; Luo, K.; Zhang, Z.; Yue, R.; Li, X.; Lei, M. Activation of persulfate by stability-enhanced magnetic gra-phene oxide for the removal of 2,4-dichlorophenol. *Sci. Total Environ.* **2019**, *707*, 135656. [[CrossRef](#)]
29. Qian, L.; Liu, P.; Shao, S.; Wang, M.; Zhan, X.; Gao, S. An efficient graphene supported copper salen catalyst for the activation of persulfate to remove chlorophenols in aqueous solution. *Chem. Eng. J.* **2019**, *360*, 54–63. [[CrossRef](#)]
30. Wu, S.; He, H.; Li, X.; Yang, C.; Zeng, G.; Wu, B.; He, S.; Lu, L. Insights into atrazine degradation by persulfate activation using composite of nanoscale zero-valent iron and graphene: Performances and mechanisms. *Chem. Eng. J.* **2018**, *341*, 126–136. [[CrossRef](#)]

31. Gao, Y.-Q.; Zhang, J.; Zhou, J.-Q.; Li, C.; Gao, N.-Y.; Yin, D.-Q. Persulfate activation by nano zero-valent iron for the degradation of metoprolol in water: Influencing factors, degradation pathways and toxicity analysis. *RSC Adv.* **2020**, *10*, 20991–20999. [[CrossRef](#)]
32. Nidheesh, P.; Khatri, J.; Singh, T.A.; Gandhimathi, R.; Ramesh, S. Review of zero-valent aluminium based water and wastewater treatment methods. *Chemosphere* **2018**, *200*, 621–631. [[CrossRef](#)] [[PubMed](#)]
33. Oh, S.-Y.; Kang, S.-G.; Chiu, P.C. Degradation of 2,4-dinitrotoluene by persulfate activated with zero-valent iron. *Sci. Total Environ.* **2010**, *408*, 3464–3468. [[CrossRef](#)] [[PubMed](#)]
34. Oh, S.-Y.; Kim, H.-W.; Park, J.-M.; Park, H.-S.; Yoon, C. Oxidation of polyvinyl alcohol by persulfate activated with heat, Fe²⁺, and zero-valent iron. *J. Hazard. Mater.* **2009**, *168*, 346–351. [[CrossRef](#)]
35. Arslan-Alaton, I.; Olmez-Hanci, T.; Korkmaz, G.; Sahin, C. Removal of iopamidol, an iodinated X-ray contrast medium, by zero-valent aluminum-activated H₂O₂ and S₂O₈²⁻. *Chem. Eng. J.* **2017**, *318*, 64–75. [[CrossRef](#)]
36. Montazeri, B.; Ucun, O.K.; Arslan-Alaton, I.; Olmez-Hanci, T. UV-C-activated persulfate oxidation of a commercially important fungicide: Case study with iprodione in pure water and simulated tertiary treated urban wastewater. *Environ. Sci. Pollut. Res.* **2020**. [[CrossRef](#)]
37. Karci, A.; Arslan-Alaton, I.; Bekbolet, M.; Ozhan, G.; Alpertunga, B. H₂O₂/UV-C and Photo-Fenton treatment of a nonylphenol polyethoxylate in synthetic freshwater: Follow-up of degradation products, acute toxicity and genotoxicity. *Chem. Eng. J.* **2014**, *241*, 43–51. [[CrossRef](#)]
38. Ucun, O.K.; Montazeri, B.; Arslan-Alaton, I.; Olmez-Hanci, T. Degradation of 3,5-dichlorophenol by UV-C photolysis and UV-C-activated persulfate oxidation process in pure water and simulated tertiary treated urban wastewater. *Environ. Technol.* **2020**, *2020*, 1–12. [[CrossRef](#)]
39. Kreuger, J. Pesticides in stream water within an agricultural catchment in southern Sweden, 1990–1996. *Sci. Total Environ.* **1998**, *216*, 227–251. [[CrossRef](#)]
40. Stamatis, N.; Hela, D.; Konstantinou, I. Occurrence and removal of fungicides in municipal sewage treatment plant. *J. Hazard. Mater.* **2010**, *175*, 829–835. [[CrossRef](#)]
41. Bessergenev, V.; Mateus, M.; Morgado, I.; Hantusch, M.; Burkel, E. Photocatalytic reactor, CVD technology of its preparation and water purification from pharmaceutical drugs and agricultural pesticides. *Chem. Eng. J.* **2017**, *312*, 306–316. [[CrossRef](#)]
42. Lopez-Alvarez, B.; Villegas-Guzman, P.; Peñuela, G.A.; Torres-Palma, R.A. Degradation of a Toxic Mixture of the Pesticides Carbofuran and Iprodione by UV/H₂O₂: Evaluation of Parameters and Implications of the Degradation Pathways on the Synergistic Effects. *Water Air Soil Pollut.* **2016**, *227*, 1–13. [[CrossRef](#)]
43. Lassalle, Y.; Jellouli, H.; Ballerini, L.; Souissi, Y.; Nicol, É.; Bourcier, S.; Bouchonnet, S. Ultraviolet-vis degradation of iprodione and estimation of the acute toxicity of its photodegradation products. *J. Chromatogr. A* **2014**, *1371*, 146–153. [[CrossRef](#)]
44. Schwack, W.; Bourgeois, B.; Walker, F. Fungicides and photochemistry photodegradation of the dicarboximide fungicide iprodione. *Chemosphere* **1995**, *31*, 2993–3000. [[CrossRef](#)]
45. Hussain, I.; Zhang, Y.; Huang, S. Degradation of aniline with zero-valent iron as an activator of persulfate in aqueous solution. *RSC Adv.* **2014**, *4*, 3502–3511. [[CrossRef](#)]
46. Hussain, I.; Zhang, Y.; Huang, S.; Du, X. Degradation of *p*-chloroaniline by persulfate activated with zero-valent iron. *Chem. Eng. J.* **2012**, *203*, 269–276. [[CrossRef](#)]
47. Messele, S.A.; Bengoa, C.; Stüber, F.E.; Giral, J.; Fortuny, A.; Fabregat, A.; Font, J. Enhanced Degradation of Phenol by a Fenton-Like System (Fe/EDTA/H₂O₂) at Circumneutral pH. *Catalysts* **2019**, *9*, 474. [[CrossRef](#)]
48. International Organization for Standardization (ISO). *Water Quality—Application of Inductively Coupled Plasma Mass Spectrometry (ICP-MS)—Part 2: Determination of 62 Elements; 17294-2*; International Organization for Standardization: Geneva, Switzerland, 2003.
49. Villegas, E.; Pomeranz, Y.; Shellenberger, J. Colorimetric determination of persulfate with alcian blue. *Anal. Chim. Acta* **1963**, *29*, 145–148. [[CrossRef](#)]
50. Bokare, A.D.; Choi, W. Zero-valent aluminum for oxidative degradation of aqueous organic pollutants. *Environ. Sci. Technol.* **2009**, *43*, 7130–7135. [[CrossRef](#)]
51. Arslan-Alaton, I.; Olmez-Hanci, T.; Ozturk, T. Effect of inorganic and organic solutes on zero-valent aluminum-activated hydrogen peroxide and persulfate oxidation of bisphenol A. *Environ. Sci. Pollut. Res.* **2018**, *25*, 34938–34949. [[CrossRef](#)] [[PubMed](#)]
52. Zhao, L.; Ji, Y.; Kong, D.; Lu, J.; Zhou, Q.; Yin, X. Simultaneous removal of bisphenol A and phosphate in zero-valent iron activated persulfate oxidation process. *Chem. Eng. J.* **2016**, *303*, 458–466. [[CrossRef](#)]
53. Arslan-Alaton, I.; Olmez-Hanci, T.; Dogan, M.; Ozturk, T. Zero-valent aluminum-mediated degradation of Bisphenol A in the presence of common oxidants. *Water Sci. Technol.* **2017**, *76*, 2455–2464. [[CrossRef](#)]
54. Temiz, K.; Olmez-Hanci, T.; Arslan-Alaton, I. Zero-valent iron-activated persulfate oxidation of a commercial alkyl phenol polyethoxylate. *Environ. Technol.* **2016**, *37*, 1–11. [[CrossRef](#)]
55. Ren, T.; Yang, S.; Jiang, Y.; Sun, X.; Zhang, Y. Enhancing surface corrosion of zero-valent aluminum (ZVAL) and electron transfer process for the degradation of trichloroethylene with the presence of persulfate. *Chem. Eng. J.* **2018**, *348*, 350–360. [[CrossRef](#)]
56. Pignatello, J.J.; Oliveros, E.; Mackay, A. Advanced Oxidation Processes for Organic Contaminant Destruction Based on the Fenton Reaction and Related Chemistry. *Crit. Rev. Environ. Sci. Technol.* **2006**, *36*, 1–84. [[CrossRef](#)]
57. Ni Soon, A.; Hameed, B. Heterogeneous catalytic treatment of synthetic dyes in aqueous media using Fenton and photo-assisted Fenton process. *Desalination* **2011**, *269*, 1–16. [[CrossRef](#)]

58. Barzegar, G.; Jorfi, S.; Zarezade, V.; Khatebasreh, M.; Mehdipour, F.; Ghanbari, F. 4-Chlorophenol degradation using ultrasound/peroxymonosulfate/nanoscale zero valent iron: Reusability, identification of degradation intermediates and potential application for real wastewater. *Chemosphere* **2018**, *201*, 370–379. [[CrossRef](#)] [[PubMed](#)]
59. Wei, X.; Gao, N.; Li, C.; Deng, Y.; Zhou, S.; Li, L. Zero-valent iron (ZVI) activation of persulfate (PS) for oxidation of bentazon in water. *Chem. Eng. J.* **2016**, *285*, 660–670. [[CrossRef](#)]
60. Zhao, J.; Zhang, Y.; Quan, X.; Chen, S. Enhanced oxidation of 4-chlorophenol using sulfate radicals generated from zero-valent iron and peroxydisulfate at ambient temperature. *Sep. Purif. Technol.* **2010**, *71*, 302–307. [[CrossRef](#)]
61. Zhang, H.; Cao, B.; Liu, W.; Lin, K.; Feng, J. Oxidative removal of acetaminophen using zero valent aluminum-acid system: Efficacy, influencing factors, and reaction mechanism. *J. Environ. Sci.* **2012**, *24*, 314–319. [[CrossRef](#)]
62. Liu, W.; Zhang, H.; Cao, B.; Lin, K.; Gan, J. Oxidative removal of bisphenol A using zero valent aluminum–acid system. *Water Res.* **2011**, *45*, 1872–1878. [[CrossRef](#)]
63. Li, H.; Wan, J.; Ma, Y.; Huang, M.; Wang, Y.; Chen, Y. New insights into the role of zero-valent iron surface oxidation layers in persulfate oxidation of dibutyl phthalate solutions. *Chem. Eng. J.* **2014**, *250*, 137–147. [[CrossRef](#)]
64. Wittke, K.; Hajimiragha, H.; Dunemann, L.; Begerow, J. Determination of dichloroanilines in human urine by GC–MS, GC–MS–MS, and GC–ECD as markers of low-level pesticide exposure. *J. Chromatogr. B Biomed. Sci. Appl.* **2001**, *755*, 215–228. [[CrossRef](#)]
65. Turci, R.; Barisano, A.; Balducci, C.; Colosio, C.; Minoia, C. Determination of dichloroanilines in human urine by gas chromatography/mass spectrometry: Validation protocol and establishment of Reference Values in a population group living in central Italy. *Rapid Commun. Mass Spectrom.* **2006**, *20*, 2621–2625. [[CrossRef](#)]
66. Fu, Y.; Gao, X.; Geng, J.; Li, S.; Wu, G.; Ren, H. Degradation of three nonsteroidal anti-inflammatory drugs by UV/persulfate: Degradation mechanisms, efficiency in effluents disposal. *Chem. Eng. J.* **2019**, *356*, 1032–1041. [[CrossRef](#)]
67. Luo, H.; Zeng, Y.; He, D.; Pan, X. Application of iron-based materials in heterogeneous advanced oxidation processes for wastewater treatment: A review. *Chem. Eng. J.* **2021**, *407*, 127191. [[CrossRef](#)]